Guidance Laws based on Optimal Feedback Linearization Pseudo-Control with Time-to-go Estimation

David Alkaher[1] and Amiram Moshaiov [2]
The Iby and Aladar Fleischman Faculty of Engineering, Tel-Aviv University, Israel

Yizhar Or[3]
Faculty of Mechanical Engineering, Technion Institute of Technology, Haifa, Israel

I. Introduction

THIS study deals with the planar Non-Linear (NL) problem of an aerial interceptor pursuing an evasive target. The pursuit problem is characterized with bounded maneuverability and constant speeds, for both interceptor and target. An ideal interceptor is considered (i.e., zero-lag dynamics). The problem is addressed for cases in which standard linearization techniques cannot be performed to simplify the equation-of-motions due to a large deviation from the nominal collision course geometry.

Many classical planar guidance strategies, such as Proportional Navigation (PN) and its variants, implement parallel navigation since it is economic in its usage of energy. PN variants, such as Pure-PN and True-PN, consist of amplifying the relative Line-Of-Sight (LOS) angular velocity. Details on such methods can be found in [1]. Modern planar guidance strategies are based on either differential-game theory (see [2]) or Optimal Control (OC) theory approaches (see [3]). These commonly involve linearization around the LOS axis. Linear Quadratic (LQ) differential-game theory was used in [2] to prove that PN (with guidance gain of N'=3) is an optimal solution to the minimum energy problem of pursuing a non-maneuvering target in the plane, under linearization. The Zero-Effort-Miss (ZEM) technique was introduced and applied in [2] to simplify the linearized equations into a scalar representation.

One option to solve the non-linearized pursuit problem is to use the Feedback Linearization (FL) method as introduced in the early 90's (e.g., [4-5]). This method transforms a NL model into an equivalent controllable linear model (see review in [6]). In contrast to [4-5], here the FL method is applied for OC. Two FL approaches are

[1] PhD student, The Iby and Aladar Fleischman Faculty of Engineering, email: dalkaher@gmail.com
[2] Senior Lecturer, The Iby and Aladar Fleischman Faculty of Engineering, email: moshaiov@eng.tau.ac.il
[3] Assistant Professor, Faculty of Mechanical Engineering, email: izi@tx.technion.ac.il

suggested. The first is based, as in [5], on the relative range. The second uses the LOS state-variable, as detailed below.

Currently there is no closed-form optimal solution to the NL guidance problem. To circumvent the analytical obstacle it is proposed here to transform the system into an equivalent linearized-form first order new system. Optimization is employed using direct and indirect costs. The later are based on the correlation between the NL guidance and its equivalent linearized form FL-based pseudo-controller. Novel closed-loop Guidance Laws (GLs), using LQ optimal pseudo-controllers with time-to-go estimation, are proposed and compared. This results with two optimal GLs, based on range and LOS.

In the next section, scalar formulation technique of the planar NL pursuit problem is presented. The optimal guidance laws are introduced in section III. Next, in section IV, an analysis of the suggested laws is presented, including a discussion on physical aspects, optimality and singularity. Finally, the conclusions are summarized in section V.

II. Scalarization of the Planar Non-linear Pursuit Problem

In subsection 'A' the kinematics of the problem are described. In subsection 'B' two alternative third-order NL system models are detailed. In subsection 'C' two corresponding equivalent-linear systems are presented using the FL technique. Finally, in subsection 'D', the ZEM technique is applied to reduce each of the systems into a single scalar differential equation, using time-to-go estimation.

A. Kinematics

The planar engagement geometry between an intercepting missile and an evading target is plotted in Fig. 1.

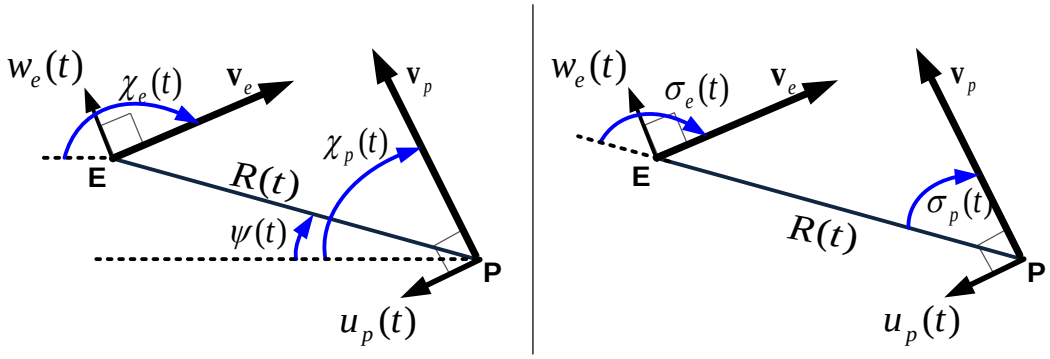

Fig. 1 Planar engagement geometry with respect to the initial LOS axis (left) and current LOS axis (right)

The instantaneous rotation angle $\psi(t)$ of the LOS is measured with respect to the initial engagement geometry. $R(t)$ is the instantaneous range between the objects. $\chi_p(t)$ and $\chi_e(t)$ are the horizontal trajectory-angles of the interceptor and the target, respectively. The bearing and aspect velocity angles, denoted by $\sigma_p(t)$ and $\sigma_e(t)$, are defined by the inner angle generated between the velocity vector and the instantaneous LOS axis (i.e., $\sigma_p(t) = \chi_p(t) - \psi(t)$ and $\sigma_e(t) = \chi_e(t) - \psi(t)$). $u_p(t)$ and $w_e(t)$ are the bounded interceptor and target controllers, respectively, (i.e., $|u_p(t)| \le 1, |w_e(t)| \le 1$). These controllers are responsible for $\dot{\chi}_p(t)$ and $\dot{\chi}_e(t)$, which are physically limited. v_p and v_e are the constant speeds of the interceptor and evading target, respectively. To simplify notations, t is omitted in the following, unless needed for clarity. The rates of the range and of the LOS angle are:

$$\begin{aligned} \dot{R} &= -v_p \cos(\sigma_p) + v_e \cos(\sigma_e) \\ \dot{\psi} &= \left[-v_p \sin(\sigma_p) + v_e \sin(\sigma_e) \right] R^{-1} \end{aligned} \tag{1}$$

B. Non Linear Third-order System Models

Two alternatives for NL third-order system representations are presented. These are given in Eq. (3) and Eq. (4) with respect to the following general-form system:

$$\dot{\mathbf{x}}_{j,pe} = f\left(\mathbf{x}_{j,pe}\right) + g\left(\mathbf{x}_{j,pe}\right) u_p + h\left(\mathbf{x}_{j,pe}\right) w_e, \quad \mathbf{x}_{j,pe} \in \Re^3, \; j \in R, \psi \tag{2}$$

The first alternative is:

$$\dot{\mathbf{x}}_{R,pe} = \begin{bmatrix} \dot{R} \\ \dot{\sigma}_e \\ \dot{\sigma}_p \end{bmatrix} = \begin{bmatrix} -v_p \cos(\sigma_p) + v_e \cos(\sigma_e) \\ -f_{\dot{\psi}} \\ -f_{\dot{\psi}} \end{bmatrix} + \begin{bmatrix} 0 \\ g v_e^{-1} n_e \\ 0 \end{bmatrix} w_e + \begin{bmatrix} 0 \\ 0 \\ g v_p^{-1} n_p \end{bmatrix} u_p, \quad \mathbf{x}_{R,pe} \in \Re^3 \tag{3}$$

In the first alternative $\dot{\psi}$ is not a state, but rather a calculated variable. On the other hand, in the second alternative, which is described in Eq. (4) below, it is a state. To distinguish between a state and a calculated variable, the later is

written as a function of the above states (i.e., $f_{\dot{\psi}} = \dot{\psi}\left(R, \sigma_p, \sigma_e\right)$). Where n_p and n_e are the maximal load factors of the interceptor and target, respectively. g is the constant of gravity.

The second alternative is:

$$\dot{\mathbf{x}}_{\psi,pe} = \begin{bmatrix} \dot{\psi} \\ \dot{\sigma}_e \\ \dot{\sigma}_p \end{bmatrix} = \begin{bmatrix} \left[-v_p \sin(\sigma_p) + v_e \sin(\sigma_e)\right] f_R^{-1} \\ -\dot{\psi} \\ -\dot{\psi} \end{bmatrix} + \begin{bmatrix} 0 \\ g v_e^{-1} n_e \\ 0 \end{bmatrix} w_e + \begin{bmatrix} 0 \\ 0 \\ g v_p^{-1} n_p \end{bmatrix} u_p, \quad \mathbf{x}_{\psi,pe} \in \Re^3 \tag{4}$$

Similarly to the first alternative, here, $\dot{R}$ and R are used as calculated variables (i.e., $f_{\dot{R}} = \dot{R}\left(\psi, \sigma_p, \sigma_e\right), f_R = \int_0^t f_{\dot{R}} dt = R$).

The output of the third-order system is defined as the instantaneous range and the LOS angle, for the first and second alternative, respectively. When the evading controller is assumed to be nulled, the general-form of the above equations is:

$$\dot{\mathbf{x}}_{j,pe} = f\left(\mathbf{x}_{j,pe}\right) + g\left(\mathbf{x}_{j,pe}\right) u_p, \quad \mathbf{x}_{j,pe} \in \Re^3, j \in R, \psi_{pe} \tag{5}$$

C. Equivalent Feedback Linearized Second-order Systems

In the following, Eq. (3) and Eq. (4) are re-formulated into equivalent linear systems by the FL method. Two approaches are examined: one involving the range (1st approach, same as in [5]), and the other involving the LOS angle (2nd approach).The equivalent-linear systems of Eq. (3) and Eq. (4), have the following general-form:

$$\dot{\mathbf{y}}_{pe} = \mathbf{A}_{pe}\mathbf{y}_{pe} + \mathbf{B}_{pe}\mu_{pe} \qquad \mathbf{A}_{pe} = \begin{bmatrix} 0 & 1 \\ 0 & 0 \end{bmatrix}, \mathbf{B}_{pe} = \begin{bmatrix} 0 \\ 1 \end{bmatrix}, \mathbf{y}_{pe} = \begin{bmatrix} y_1 \\ y_2 \end{bmatrix} \in \Re^2 \tag{6}$$

In the above general-form the FL state-vector and the pseudo-controller are denoted by $\mathbf{y}_{pe}$ and μ_{pe}, respectively. It is specifically denoted by the subscripts $_{pe,R}$ and $_{pe,\psi}$, as follows:

$$1^{st} \text{ approach: } \mu_{pe,R} \equiv \ddot{R}, \quad \mathbf{y}_{pe,R} = \begin{bmatrix} R \\ \dot{R} \end{bmatrix} \tag{7}$$

$$2^{nd} \text{ approach: } \mu_{pe,\psi} \equiv \ddot{\psi}, \quad \mathbf{y}_{pe,\psi} = \begin{bmatrix} \psi \\ \dot{\psi} \end{bmatrix} \tag{8}$$

The equivalent linear system of the first approach involves a pseudo-controller that influences the interception range. In the second approach, the pseudo-controller influences the LOS angle.

D. Equivalent First-order System

A novel Zero-Effort-Feedback (ZEF) variable is derived. The well-known ZEM technique is applied on Eq. (6), to further reduce the equivalent system into the following scalar representation:

$$Z^{OC}_{Feedback}(t) = \begin{bmatrix} 1 & 0 \end{bmatrix} \boldsymbol{\varphi}(t_f, t) \mathbf{B} \mu_{pe} = t_{go} \mu_{pe} \tag{9}$$

Where $\boldsymbol{\varphi}(t_f, t)$ is the state transition matrix, associated with the homogeneous system $\dot{\mathbf{y}} = \mathbf{A}\mathbf{y}$, and defined as follows: $\boldsymbol{\varphi}(t_f, t) = \begin{bmatrix} 1 & t_{go} \\ 0 & 1 \end{bmatrix}$. $Z^{OC}_{Feedback}$ is the resulting ZEF scalar variable. t_{go} is the remaining time-to-go till rendezvous (i.e., $t_{go} = t_f - t$). The ZEF variable, presented in Eq. (9), can be calculated as follows:

$$Z^{OC}_{feedback}(t) = \begin{bmatrix} 1 & 0 \end{bmatrix} \boldsymbol{\varphi}(t_f, t) \mathbf{y}(t) = y_1 + t_{go} y_2 \tag{10}$$

The ZEF variable holds a physical meaning since it represents the anticipated terminal miss-distance (1st approach) or the anticipated terminal LOS angle (2nd approach), if from the current time onwards the pursuit controller is activated such that it maintains a zero-value to the pseudo-controller. The general notation $Z_{Feedback}^{OC}$ is eplaced with, Z_{FM}^{OC}, Z_{FA}^{OC} , for the 1st (Feedback Miss) and 2nd (Feedback Angle) approaches, respectively. These are detailed in Table 1.

Table 1. ZEF Variable Values, Calculated for Both FL Approaches

Approach	ZEF variable value
Range-based 1st approach : $\mu_{pe,R} \equiv \ddot{R}$, $\mathbf{y}_{pe,R} = \begin{bmatrix} R \\ \dot{R} \end{bmatrix}$	$Z_{FM}^{OC} = R + t_{go}\dot{R}$ Distance of miss assuming zero-value pseudo-controller is maintained from the current time onwards
LOS-based 2nd approach : $\mu_{pe,\psi} \equiv \ddot{\psi}$, $\mathbf{y}_{pe,\psi} = \begin{bmatrix} \psi \\ \dot{\psi} \end{bmatrix}$	$Z_{FA}^{OC} = \psi + t_{go}\dot{\psi}$ Expected final LOS angle, at rendezvous, assuming zero-value pseudo-controller is maintained

To estimate the time-to-go, at each step of the calculations, it is suggested to use the analytical expression from [7], as given in Eq. (11). It describes the remaining time until rendezvous, assuming that both interceptor and target will not employ any controls (i.e., zero-effort), from now on. It is hereby referred to as the zero-effort time-to-go.

$$t_{go} = -\frac{R\dot{R}}{\dot{R}^2 + R^2\dot{\psi}^2} \tag{11}$$

III. Optimal Feedback Linearization Guidance Laws

There exists an analytical relation between the guidance (physical) controller and the pseudo-controller, which is presented in subsection 'A'. In subsection 'B' a ZEF-based LQ optimization problem is defined, for each approach, and solved for the optimal pseudo-controller and the associated guidance controller.

A. Extracting the Guidance Controllers from the Pseudo- Controllers

The relationships between the pseudo-controllers $\left(\mu_{pe,R}, \mu_{pe,\psi}\right)$ and the physical controllers $\left(u_p, w_e\right)$ are presented (for each approach) by diagrams in Table 2. The pseudo-controllers (shown in Table 2) result from a time derivative of the range and LOS state variable rates that are given in Eq. (1). It is noted that since a zero-lag interceptor-dynamics is considered, the achieved and the command acceleration are equal.

Table 2 Relationships Between the Pseudo and the Guidance Controllers

	1st approach	2nd approach
	$\mu_{pe,R} = \ddot{R} = gn_p \sin(\sigma_p)u_p + gn_e \sin(\sigma_e)w_e + f_{\dot{\psi}}^2 R$	$\mu_{pe,\psi} = \ddot{\psi} = -gn_p \cos(\sigma_p) f_R^{-1} u_p + gn_e \cos(\sigma_e) f_R^{-1} w_e - 2\dot{\psi} f_{\dot{R}} f_R^{-1}$
Diagrams for calculating the guidance controller	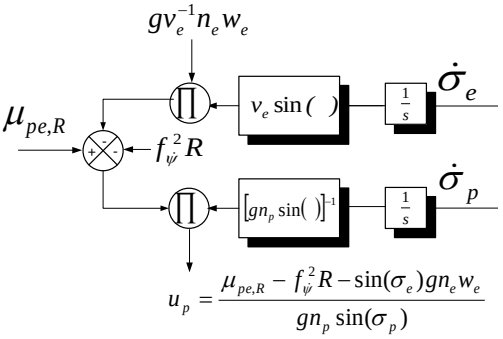	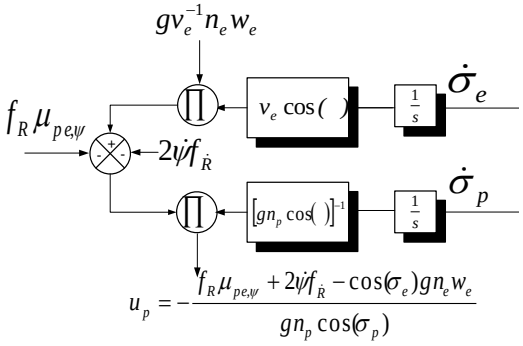

The target strategy may be known to the interceptor (in this case an augmented guidance law can be derived) or unknown (in this case a non-maneuvering target is assumed). In the rest of this study the value of the evading controller is nulled (target strategy is considered unknown).

B. Feedback Linearization Optimization

i. General formulation

Legitimate design goals for extracting a guidance strategy are minimizing the miss distance or aiming for a required LOS angle at rendezvous, while minimizing the 'control-effort' of the guidance controller (i.e., $\int_0^{t_f} u_p^2 dt$). The required LOS angle is denoted by $\psi_{req}(t_f)$. It is shown here that dictating the final LOS to be equal to the intial one, such that $\psi_{req}(t_f) = \psi(t_0)$, can encourage parallel navigation. In Table 3, the well-known LQ cost function (see [3]) is used to describe these goals as a weighted-sum of two quadratic terms (where ρ, κ are positive coefficients):

Table 3 LQ Cost Functions for the Desired Guidance Strategy Goals

Minimizing the miss distance	Aiming for a required LOS angle at rendezvous
$J = \frac{\rho}{2}\left[R(t_f)\right]^2 + \frac{\kappa}{2}\int_0^{t_f} u_p^2 dt$	$J = \frac{\rho}{2}\left[\psi(t_f) - \psi_{req}(t_f)\right]^2 + \frac{\kappa}{2}\int_0^{t_f} u_p^2 dt$

ii. Proposed Zero-Effort-Feedback based cost formulation

An analytical solution for the formulation of Table 3, using Eq. (3) or Eq. (4), is not available. An alternative method, with modified costs, is suggested hereby for solving the guidance strategies. Direct and indirect costs are defined based on the relationships in Table 2. The direct part consists of optimizing the required value of the relative distance or the LOS angle at rendezvous. The direct part is possible since the ZEF variable of the 1st and 2nd approach ($Z_{FM}^{OC}(t), Z_{FA}^{OC}(t)$), are equal to the relative distance and LOS angle at rendezvous, respectively (i.e., $R(t_f)$ and $\psi(t_f)$). The indirect part consists of an implicit minimization of the guidance control by minimizing the related effort of the pseudo-control ($\int_0^{t_f} \mu_{pe}^2 dt$). Thus, an alternative ZEF-based LQ cost is suggested (in accordance with Table 3) in Table 4:

Table 4 LQ Cost Functions for Solving the Optimal Pseudo-controllers

Minimizing the miss distance (1st approach)	Aiming for a required LOS angle at rendezvous (2nd approach)
$J=\frac{\rho}{2}\left[Z_{FM}^{OC}(t_f)\right]^2+\frac{\kappa}{2}\int_0^{t_f}\mu_{pe,R}^2 dt$	$J=\frac{\rho}{2}\left[Z_{FA}^{OC}(t_f)-\psi_{req}(t_f)\right]^2+\frac{\kappa}{2}\int_0^{t_f}\mu_{pe,\psi}^2 dt$

iii. Optimal-feedback-linearization-based guidance laws

There exists a closed-loop (global) optimal solution to the LQ problem of Table 4 that satisfies Eq. (9), (e.g., see [3]). Explicit optimal pseudo-controllers are given in Eq. (12), which are derived by substituting the $Z_{Feedback}^{OC}$ expression of each approach (i.e., Z_{FM}^{OC} or Z_{FA}^{OC} for the 1st and 2nd approach, respectively), within that LQ general-form closed-loop solution (see elaboration in appendix A)

$$\begin{aligned}\mu_{pe,R}^{*}&=-\frac{3Z_{FM}^{OC}t_{go}}{3\frac{\kappa}{\rho}+t_{go}^3} \qquad 1st\quad approach\\ \mu_{pe,\psi}^{*}&=-\frac{3\left[Z_{FA}^{OC}-\psi_{req}(t_f)\right]t_{go}}{3\frac{\kappa}{\rho}+t_{go}^3} \quad 2nd\quad approach\end{aligned} \tag{12}$$

Three special cases are discussed. These are shown in the Table 5. In the middle-column the costs for the special cases are detailed. Based on the explicit optimal pseudo-controllers and the working relationships, which are presented in Table 2, the associated GLs are derived and presented in the right-column of Table 5.

The resulting analytic expressions of Table 5 are simple to implement. The GL, based on the 1st approach, is denoted by R-OFL-GL (Range-based Optimal-FL-based GL). The other two GLs are based on the 2nd approach, including: True-PN, when $\kappa\to\infty$, and P-OFL-GL (Parallel-Optimal-FL-based GL), when $\psi_{req}(t_f)=\psi(t_0)$. The physical aspects, the singularities, and the optimization aspects of these GLs are discussed below in section IV.

Table 5 Non Linear Optimal-FL-based GL

Guidance Law Name	Cost Optimal Feedback Linearization Control	Guidance Law u_p
R-OFL-GL	$J = \frac{\rho}{2}\left[Z_{FM}^{OC}(t_f)\right]^2 + \frac{\kappa}{2}\int_0^{t_f} \mu_{pe,R}^2 dt$ $\rho \to \infty,\ \kappa > 0$ (i.e., the objective to achieve zero miss is the significant objective) $\mu_{pe,R}^* = -3\frac{R + \dot{R}t_{go}}{t_{go}^2}$	$\frac{\mu_{pe,R}^* - f_\psi^2 R}{g n_p \sin\left[\sigma_p\right]}$
True-PN	$J = \frac{\rho}{2}\left[Z_{FA}^{OC}(t_f) - \psi_{req}(t_f)\right]^2 + \frac{\kappa}{2}\int_0^{t_f} \mu_{pe,\psi}^2 dt$ $\kappa \to \infty$ $\mu_{pe,\psi}^* = 0$	$-\frac{2\dot{\psi} f_{\dot{R}}}{n_p g \cos\left[\sigma_p\right]}$
P-OFL-GL	$J = \frac{\rho}{2}\left[Z_{FA}^{OC}(t_f) - \psi_{req}(t_f)\right]^2 + \frac{\kappa}{2}\int_0^{t_f} \mu_{pe,\psi}^2 dt$ $0 < \rho < \kappa,\ \psi_{req}(t_f) = \psi(t_0)$ $\mu_{pe,\psi}^* = -\frac{3\left[\psi - \psi(t_0) + \dot{\psi}t_{go}\right]t_{go}}{3\frac{\kappa}{\rho} + t_{go}^3}$	$-\frac{f_R \mu_{pe,\psi}^* + 2\dot{\psi} f_{\dot{R}}}{n_p g \cos\left[\sigma_p\right]}$

IV. Discussion

It can be easily shown that the first guidance strategy, $u_p\left(\mu^*_{pe,R}\right)$, resulting from R-OFL-GL (which is obtained when $\rho \to \infty$), is optimal. In this case the goal of minimizing the pseudo-controller effort is omitted. Hence, in this degenerated case the resulting guidance strategy is also optimal. Similarly, it can be shown that when $\kappa \to \infty$ it results in the optimal GL of True-PN with N'=2 (proved for optimality in [8]). Third, when $\psi_{req}(t_f) = \psi(t_0)$, the guidance strategy, $u_p\left(\mu^*_{pe,\psi}\right)$, results with parallel navigation guidance-implementation. The rest of this paper concentrates on R-OFL-GL and P-OFL-GL. Further discussion on the optimization aspects of these guidance strategies is given in appendix B.

Considering a rotating frame of reference that is attached to the interceptor, two fictitious forces are observed. The first is the 'centrifugal force', $f_{\dot{\psi}}^2 R$, which is directed along the LOS axis. The second is the 'Coriolis force', $2\dot{\psi}f_{\dot{R}}$, which is directed perpendicular to the LOS axis. Both R-OFL-GL and P-OFL-GL consist of two components. Their first component is related to the pseudo-controller, whereas their second component is related to a fictitious force (that can be observed in the rotating system). When R-OFL-GL is considered, the pursuit command is applied along the LOS axis; the fictitious force is the 'centrifugal force'. However, when P-OFL-GL is considered, the pursuit command is applied perpendicular to the LOS axis; the fictitious force is the 'Coriolis force'.

The R-OFL-GL and P-OFL-GL have singularities at $\sigma_p = [0, \pi]$ and $\sigma_p = [0.5\pi, 1.5\pi]$, respectively. Analyzing the effects of the fictitious forces (see elaboration in appendix B), leads to the following conclusions. First, when R-OFL-GL is considered, the 'centrifugal force' steers the interceptor into the problematic singularities of the bearing-angle σ_p. This causes saturation and a bang-bang effect, which maintains the bearing-angle around its singular value. When linear conditions are either satisfied or maintained (i.e., $\dot{\psi} \approx 0$, thus $R \approx -\dot{R}t_{go}$), these singularities are avoided. Second, when P-OFL-GL is considered, the 'Coriolis force' does not enforce the interceptor to converge into the problematic singularities (since it aims to maintain parallel navigation), hence singularity is avoided.

V. Conclusions

The planar Non-Linear (NL) problem of an ideal aerial-interceptor pursuing an evasive target is studied. New closed-loop analytical Optimal-Feedback-Linearization-based Guidance Laws (OFL-GLs) are proposed using Feedback Linearization (FL) and OC theory, with zero-effort time-to-go estimation. The first is Range-OFL-GL (R-OFL-GL) and the second is Parallel-OFL-GL (P-OFL-GL). The resulting strategies are discussed with respect to the obtained optimal FL pseudo-controllers . In addition, the roles of the fictitious forces (i.e., Coriolis and centrifugal) are discussed and related to the obtained singularities of the resulting guidance strategies.

Simulation results (shown in appendix C), indicate that R-OFL-GL is less efficient in terms of 'control effort', in comparison with P-OFL-GL, when the pursuit scenario starts with a collision course geometry. When starting on that geometry and when linearity is violated, R-OFL-GL strategy applies an extensive guidance effort to leave this geometry, while P-OFL-GL applies less effort to stay on it. When initial heading-errors are considered for the bearing-angle, using R-OFL-GL results with singular behavior, whereas using P-OFL-GL, does not. When large heading-errors are considered, P-OFL-GL does not guarantee capture.

VI. References

[1] Shneydor, N. A., "Parallel Navigation," *Missile Guidance and Pursuit: Kinematics, Dynamics and Control*, Horwood Publishing Limited, Chichester, 1998, pp. 77-100.

[2] Bryson, A. E., and Ho, Y. C., "Differential Games," *Applied Optimal Control: Optimization, Estimation, and Control*, Hemisphere Publishing Corporation, Washington, DC, 1975, pp. 282-289.

[3] Ben-Asher, J., and Yaesh, I., "Optimal Guidance Based on Linear-Quadratic One-Sided Optimization," *Advances in Missile Guidance Theory*, edited by P. Zarchan, Vol. 180, Progress in Astronautics and Aeronautics, AIAA, Reston, Virgina, 1998, pp. 25-42.

[4] Ha, I. J., and Chong, S., "Design of CLOS Guidance Law Via Feedback Linearization," *IEEE Transactions on Aerospace and Electronic Systems*, Vol, 28, No. 1, January 1992, pp. 51-62.

doi: 10.1109/7.135432

[5] Bezick, S., Rusnak, I., and Gray, W. S., "Guidance of a Homing Missile via Nonlinear Geometric Control Methods," *Journal of Guidance, Control and Dynamics*, Vol. 18, No. 3, May-June 1995, pp. 441-448.

[6] Slotine, J.-J. E., and Li, W., "Feedback Linearization," Applied Non Linear Control, Vol. 199., No. 1., Prentice-Hall, Inc., New Jersey, 1991, pp. 229-235.

doi: 10.2514/3.21407

[7] Rawling, A. G., "Passive Determination of Homing Time," *AIAA Journal*, Vol. 6, No. 8, August 1968, pp. 1604–1606.

doi: 10.2514/3.4826

[8] Heller, C., Yaesh, I., and Ben-Asher, J., "Optimal Setting of the Proportional-Navigation Gain," Journal of Guidance, Control, and Dynamics Vol. 36, No.3, 2013, pp. 887-890.

doi: 10.2514/1.59226

VII. Appendix A. – General-form Linear-Quadratic Solution of the Optimal Pseudo-Controllers

The proposed alternative LQ ZEF-based costs, given in Table 4, are re-presented in the following general-form:

$$J = \frac{\rho}{2}\left[Z_{Feedback}^{OC}(t_f) - x_{pe}^{i,req}\right]^2 + \frac{\kappa}{2}\int_0^{t_f} \mu_{pe}^2 dt \tag{13}$$

where $Z_{Feedback}^{OC}(t)$ is the general-form notation of the relevant ZEF variable; $x_{pe}^{i,req}$ is the required value of the relevant i-th variable of the state-variable vector, described in Eq. (2); and μ_{pe} is the appropriate pseudo-controller, described in Table 4. The general-form scalar differential equation-of-motions (Eq. 9) is re-stated here as:

$$\dot{Z}_{Feedback}^{OC}(t) = t_{go}\mu_{pe} \tag{14}$$

The Hamiltonian of the problem is:

$$H = \lambda \dot{Z}_{Feedback}^{OC} + \frac{\kappa}{2}\mu_{pe}^2 = \lambda t_{go}\mu_{pe} + \frac{\kappa}{2}\mu_{pe}^2 \tag{15}$$

Thus, the adjoint equations, satisfying necessary conditions for optimality, are:

$$\dot{\lambda} = -\frac{\partial H}{\partial Z_{Feedback}^{OC}} = 0 \tag{16}$$

$$\lambda(t_f) = \frac{\partial J}{\partial Z_{Feedback}^{OC}(t_f)} = \rho\left[Z_{Feedback}^{OC}(t_f) - x_{pe}^{i,req}\right] \tag{17}$$

Yielding the following solution:

$$\lambda = \rho\left[Z_{Feedback}^{OC}(t_f) - x_{pe}^{i,req}\right] \tag{18}$$

The optimal pseudo-controller satisfies $\mu_{pe}^* = \arg_{\mu_{pe}} \min H$; thus an optimal open-loop solution can be obtained:

$$\begin{aligned} \mu_{pe}^* &= \arg_{\mu_{pe}}\left[\frac{\partial H}{\partial \mu_{pe}} = \lambda t_{go} + \kappa\mu_{pe} = 0, \quad \frac{\partial^2 H}{\partial \mu_{pe}^2} = \kappa > 0\right] \\ &= -\rho\kappa^{-1}\left[Z_{Feedback}^{OC}(t_f) - x_{pe}^{i,req}\right]t_{go} \end{aligned} \tag{19}$$

The candidate closed-loop solution of the problem can be found by integrating the single equation of motion and assigning value to the feedback command:

$$Z_{Feedback}^{OC}(t_f) = Z_{Feedback}^{OC} + \int_t^{t_f} t_{go}\mu_{pe}dt = \frac{Z_{Feedback}^{OC} + \rho\kappa^{-1}x_{pe}^{i,req}\frac{t_{go}^3}{3}}{1+\rho\kappa^{-1}\frac{t_{go}^3}{3}} \tag{20}$$

The closed-loop optimal solution is therefore:

$$\mu_{pe}^{*} = -\frac{3\left[Z_{Feedback}^{OC} - x_{pe}^{i,req}\right]t_{go}}{3\frac{\kappa}{\rho}+t_{go}^3} \tag{21}$$

VIII. Appendix B. – Discussion of Optimality

In the following the resulting strategies (listed in the right-column of Table 5) are discussed with respect to the obtained optimal FL controllers (listed in the middle-column of that table).

The first guidance strategy, $u_p\left(\mu^*_{pe,R}\right)$, resulting from R-OFL-GL when $\rho \to \infty$, is optimal. In this case the goal of minimizing the effort of the pseudo-controller is omitted. Hence, in this degenerated case the resulting guidance strategy is also optimal. The second guidance strategy, $u_p\left(\mu^*_{pe,\psi}\right)$, resulting from Eq. (12) does not use explicit requirements on the miss. This is in contrast to the costs that are usually employed when deriving optimal guidance laws. Hence, capture is not guaranteed. Yet, it can be used for practical purposes as discussed in the following two observations. The first observation is that when $\kappa \to \infty$ (i.e., $\mu^*_{pe} = 0$) is applied, the suggested guidance strategy becomes the well-known True-PN guidance strategy with gain of N'=2. The True-PN guidance strategy, with that gain, was proven in [8] to be optimal in the context of energy minimization (i.e., $\int_0^{t_f} u_p^q dt, q \to \infty$) of a linearized model problem. The second observation is that $u_p\left(\mu^*_{pe,\psi}\right)$ leads to zero-miss, when $\psi_{req}(t_f) = \psi(t_0)$ and $\rho < \kappa$ (assuming the evader does not perform any maneuvers). This case is referred to as P-OFL-GL in section III. The following provides an explanation to this statement. In the case of $\rho < \kappa$ and $\psi_{req}(t_f) = \psi(t_0)$ the LQ formulation, given in Table 5, is aiming to minimize two objectives. Looking at the first objective shows that it can be minimized to zero if $\psi(t_f) = \psi(t_0)$ is satisfied. Looking at the preferred second objective shows that it can be minimized if $\mu_{pe} = \ddot{\psi} = 0$ can be satisfied. This can be achieved if both $\psi = \psi(t_0)$ and $\dot{\psi} = 0$ are satisfied as well (as seen from the expression for the pseudo-controller in Table 5). It is important to note that both objectives are not contradicting. When both $\psi = \psi(t_0)$ and $\dot{\psi} = 0$ are satisfied, parallel navigation is generated, which is known to enforce zero-miss (under the discussed assumptions).

IX. Appendix C. – Discussion on Singularity and Simulation Results

The guidance strategies R-OFL-GL and P-OFL-GL, which are given in Table 5, have singularities at $\sigma_p = [0, \pi]$ and $\sigma_p = [0.5\pi, 1.5\pi]$, respectively. Analyzing the effect of the fictitious forces on the singularity behavior of the guidance strategies leads to the following main conclusions, which are also demonstrated by simulations.

First, when R-OFL-GL is considered, the 'centrifugal force' steers the interceptor into the problematic singularities of the bearing-angle σ_p (i.e., to result with head-on or tail-chase geometries). This causes saturation and a bang-bang effect. When linear conditions are satisfied these singularities are avoided. To support this claim, the following mathematical manipulation is considered, describing the relative velocities of the interceptor with respect to the origin of reference axes:

$$\begin{aligned} r_p\dot{\psi} &= v_p \sin(\sigma_p) \\ \dot{r}_p &= v_p \cos(\sigma_p) \end{aligned} \tag{22}$$

Where r_p is the relative distance of the interceptor from that axes. When linearization conditions are satisfied (i.e., $\dot{\psi} \approx 0$, thus $R \approx -\dot{R}t_{go}$), it results with $\mu^*_{pe,R} = 0$ (see pseudo-controller in Table 5). Analyzing the trajectory-angle rotation rate, which is calculated by $\dot{\chi}_p = gn_p u^*_p v_p^{-1}$, shows that the singularity is avoided:

$$\dot{\chi}_p = \frac{gn_p u^*_p}{v_p} = -\frac{\dot{\psi}^2 R}{v_p \sin[\sigma_p]} = \frac{\dot{\psi}^2 R}{r_p \dot{\psi}} = \frac{\dot{\psi} R}{r_p} \tag{23}$$

Second, when P-OFL-GL is considered, the 'Coriolis force' discourages the interceptor from converging into the problematic singularities (since it aims to maintain parallel navigation). In the case of initial heading-error this may result with parallel navigation either to capture or to divergence, as typical to parallel navigation.

In the following example, R-OFL-GL and P-OFL-GL (with $\kappa:\rho=100:1$) strategies are simulated with respect to a collision-course-geometry scenario (see Fig. 2) and with respect to heading-errors (see Fig. 4). The scenarios are set for physical parameters that do not guarantee the superiority of the interceptor over the target ($\varepsilon_n = n_p n_e^{-1} = 3$, $\varepsilon_v = v_p v_e^{-1} = 2, n_e = 5, v_e = 300$). A weaving target maneuver is considered, $w_e = \sin(0.5t + \pi)$. The initial relative displacement is set to 10 kilometers. The trajectory aspect-angles are set to 120 [deg], for both scenarios. The bearing angels are constructed for each scenario with respect to the initial collision-course-geometry. In the first case (see Fig. 2) it is set with no heading-error, whereas in the second case (see Fig. 4) with a heading-error value of -60 [deg] (measured with respect to the collision-course-geometry).

The results of each simulation are presented in two plots. In the first plot (see Fig. 2 and 4) planar pursuit-trajectories (of R-OFL-GL vs. P-OFL-GL) are presented. The interceptor's trajectory starts from the origin of axis. Several LOS are added to the figure to visualize the angular change of the LOS during pursuit. In the second plot (see Fig. 3 and 5) LOS, bearing-angles and guidance controllers are depicted with respect to the time-to-go.

R-OFL-GL strategy aims to null the miss distance at rendezvous, with respect to the anticipated time-to-go. The time-to-go is extrapolated from the zero-effort-tgo expression, given in Eq. (11). Its' normalized 'control effort' is found to be greater than that of the P-OFL-GL and of the well-known PN guidance strategy (not presented). P-OFL-GL aims to implement a parallel navigation guidance strategy, by preserving the initial LOS angle. It is noticed that as long as linearized conditions are kept, the interceptors' trajectories are approximately 'straight and level' (i.e., no guidance is applied). The P-OFL-GL maintains the pursuer on linearized conditions, whereas the R-OFL-GL does not. In the later case an extensive guidance effort is applied to leave this geometry when linearization conditions are interrupted.

In the R-OFL-GL pursuit scenarios, when linearized conditions are interrupted, singularity is observed (see bearing-angle values in Fig. 3 and 5) and saturation occurs (see guidance controller values). It can be seen from the planar trajectories of R-OFL-GL (see Fig. 2) that here saturation results in a miss. In the simulated scenarios, when the load ratio is not enough to keep the R-OFL-GL interceptor's guidance-law out of saturation, P-OFL-GL is superior. It is also shown in Fig. 3 and 5 that the P-OFL-GL control-effort is maintained at lower values.

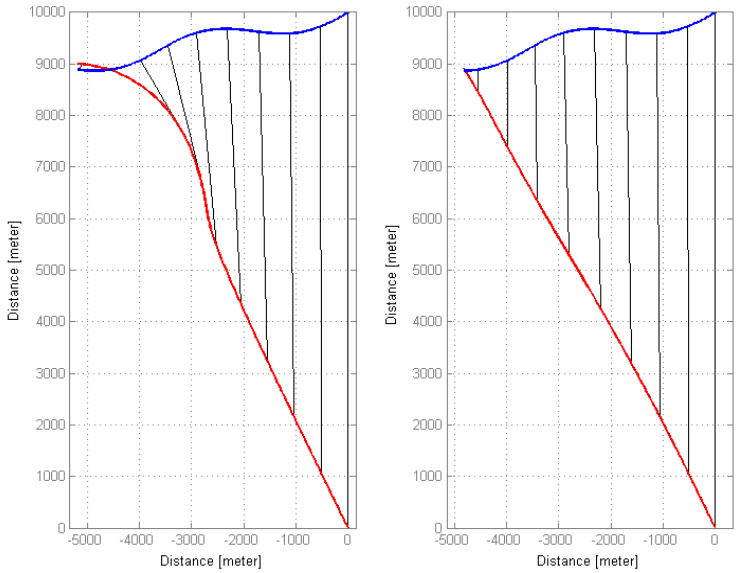

Fig. 2 Planar trajectories of R-OFL-GL (left) vs. P-OFL-GL (right) when Collision-course-geometry is set

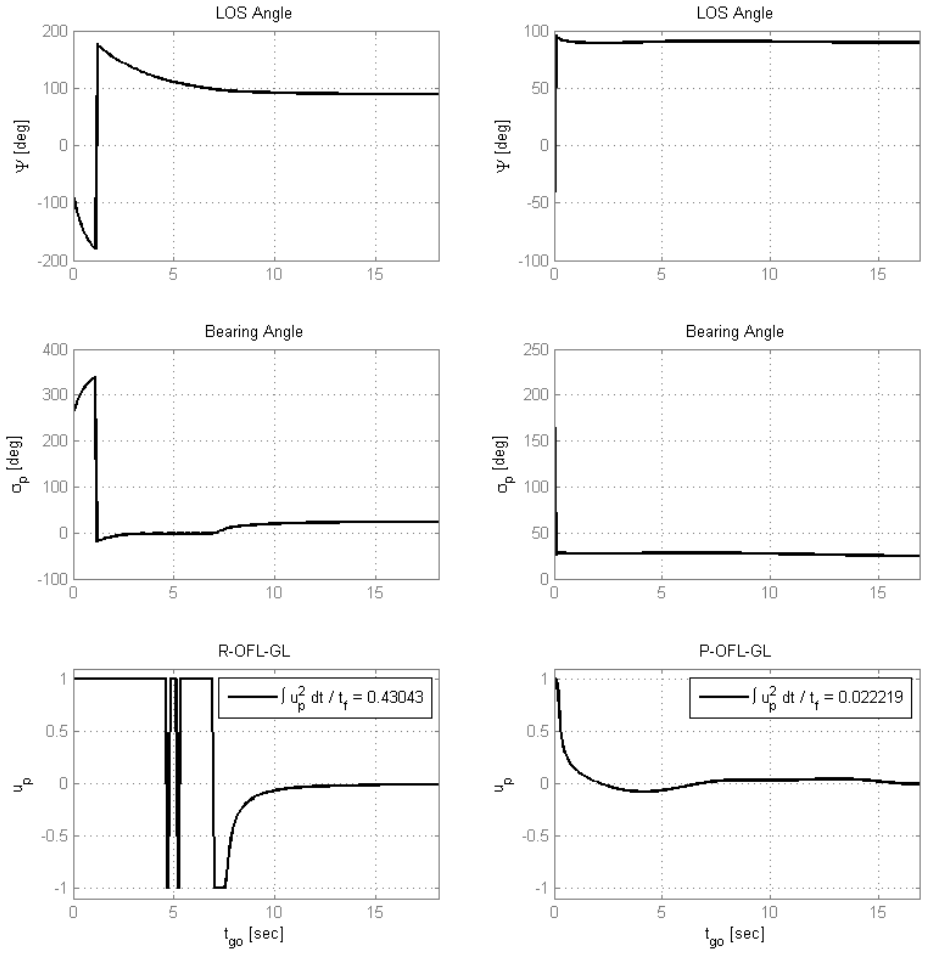

Fig. 3 LOS, bearing-angles and guidance controllers of R-OFL-GL (left) vs. P-OFL-GL (right)

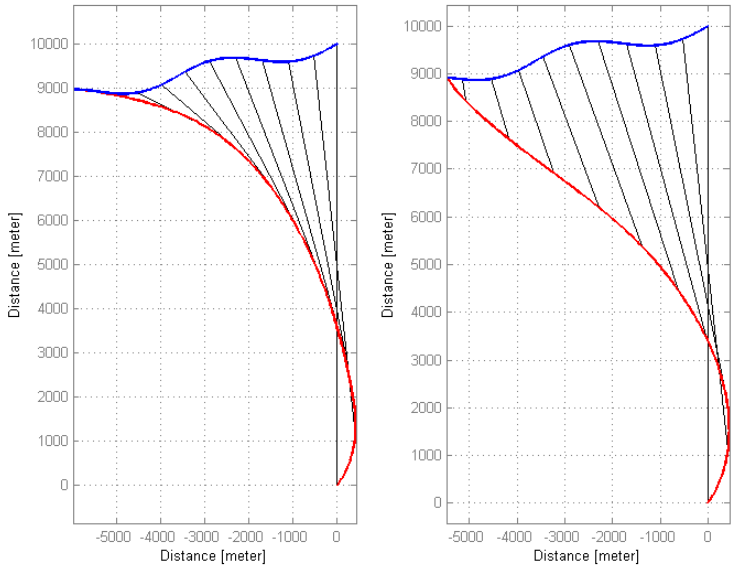

Fig. 4 Planar trajectories of R-OFL-GL (left) vs. P-OFL-GL (right) with initial heading-errors

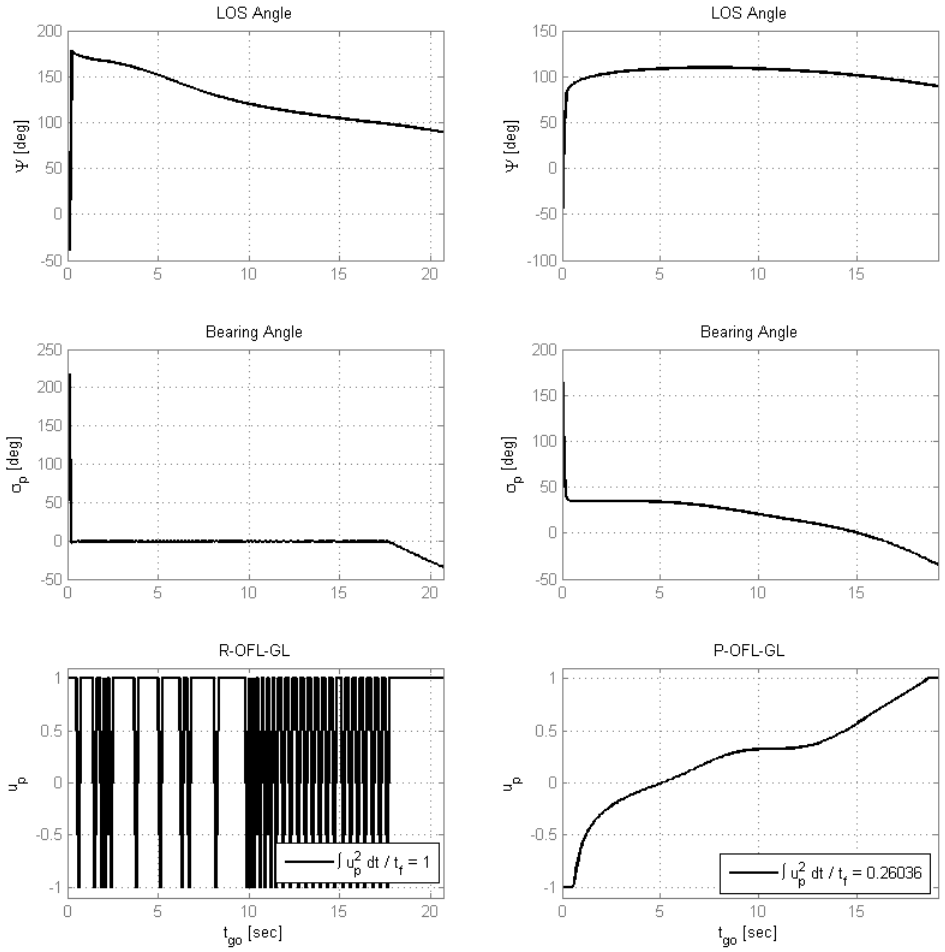

Fig. 5 LOS, bearing-angles and guidance controllers of R-OFL-GL (left) vs. P-OFL-GL (right)